Volume 64, February 2014

ISSN 0306-4549

ELSEVIER

annals of
NUCLEAR ENERGY

Special Section
Progress on Molten Salt Reactors (MSR) and Salt-cooled Reactors (FHR)

Guest Editors
Jan Leen Kloosterman, Marco E. Ricotti and Elsa Merle-Lucotte

Available online at www.sciencedirect.com

ScienceDirect

Annals of Nuclear Energy 64 (2014) 449–456

Contents lists available at ScienceDirect

Annals of Nuclear Energy

journal homepage: www.elsevier.com/locate/anucene

Preliminary thermal–hydraulic core design of the Molten Salt Fast Reactor (MSFR)

H. Rouch [a], O. Geoffroy [a], P. Rubiolo [b,*], A. Laureau [b], M. Brovchenko [b], D. Heuer [b], E. Merle-Lucotte [b]

[a] INOPRO, 118 Chemin des Breux, F-38250 Villard de Lans, France
[b] LPSC-IN2P3-CNRS/UJF/Grenoble INP, 53 rue des Martyrs, F-38026 Grenoble Cedex, France

ARTICLE INFO

Article history:
Received 18 February 2013
Accepted 3 September 2013
Available online 4 October 2013

Keywords:
MSFR
Molten salt reactor
Thermal–hydraulics design
Core cavity
CFD
Fuel salt temperature

ABSTRACT

A thermal–hydraulics study of the core of the Molten Salt Fast Reactor (MSFR) is presented. The numerical simulations were carried-out using a Computation Fluid Dynamic code. The main objectives of the thermal–hydraulics studies are to design the core cavity walls in order to increase the overall flow mixing and to reduce the temperature peaking factors in the salt and on the core walls. The results of the CFD simulations show that for the chosen core design acceptable temperature distributions can be obtained by using a curved core cavity shape, inlets and outlets. The hot spot temperature is less than 10 °C above the average core outlet temperature and is located in the centre of the top wall of the core. The results show also a moderate level of sensitivity to the working point.

1. Introduction

The Generation-IV International Forum (GIF) for the development of new nuclear energy systems has established a set of goals as research directions for nuclear systems (US DOE, 2002): enhanced safety and reliability, reduced waste generation, effective use of uranium or thorium ores, resistance to proliferation, improved economic competitiveness. Molten Salt Reactors (MSRs) are one of the systems retained by this forum in 2002. The CNRS has been involved in molten salt reactor studies since 1997. Starting from the Oak-Ridge National Laboratory Molten Salt Breeder Reactor project (Whatley et al., 1970), an innovative concept called Molten Salt Fast Reactor or MSFR (Nuttin et al., 2005; Mathieu et al., 2006, 2009; Forsberg et al., 2007; Merle-Lucotte et al., 2008, 2009) has been proposed. This concept results from extensive parametric studies in which various core arrangements, reprocessing performances and salt compositions were investigated in order to optimize the performance of a large thorium based reactor fleet.

As opposed to thermal molten salt reactors (Bettis et al., 1970), the specificity of the MSFR is the removal of the solid moderator (usually graphite) in the core which results in a fast breeder reactor with a large negative power coefficient and operated in the Thorium fuel cycle. Other important advantages of the fast spectrum include a better breeding ratio, the reduction of the reprocessing requirements and the absence graphite lifespan issues. These unique advantages for actinide burning and extending fuel resources were recognized by the Generation IV International Forum which selected in 2008 the MSFR concept as one of the GEN IV reference reactors (GIF, 2008).

The present paper is focused on the thermal–hydraulics design of the MSFR core using a Computational Fluid Dynamic code and the detailed core geometry. The main objectives of the thermal–hydraulics studies were to design the core cavity, including the fuel salt inlets and outlets, in order to:

- Increase the overall flow mixing in the core cavity.
- Reduce the temperature peaking factors in the salt and on the core walls.
- Avoid if possible the use of any core internal structure to improve flow mixing.

The aim of the first point is to improve the uniformity of the salt composition and of the distribution of inert gas bubbles used for fission product extraction (such as they are able to clean a maximum of the volume of fuel salt). Minimizing the temperature gradient of the salt helps reducing the thermal stress induced on the core wall structures. Concerning the last point, initial studies shown that core internal structures (such as perforated plates, grids or salt injectors) could be used to improve the flow distribution but will significantly increase the core pressure losses. This, and other drawbacks that are discussed in the next section, redirected the design effort to the use of the core walls as a mean to optimize the flow distribution.

* Corresponding author. Tel.: +33 476284068.
E-mail address: rubiolo@lpsc.in2p3.fr (P. Rubiolo).

0306-4549/$ - see front matter © 2013 Elsevier Ltd. All rights reserved.
http://dx.doi.org/10.1016/j.anucene.2013.09.012

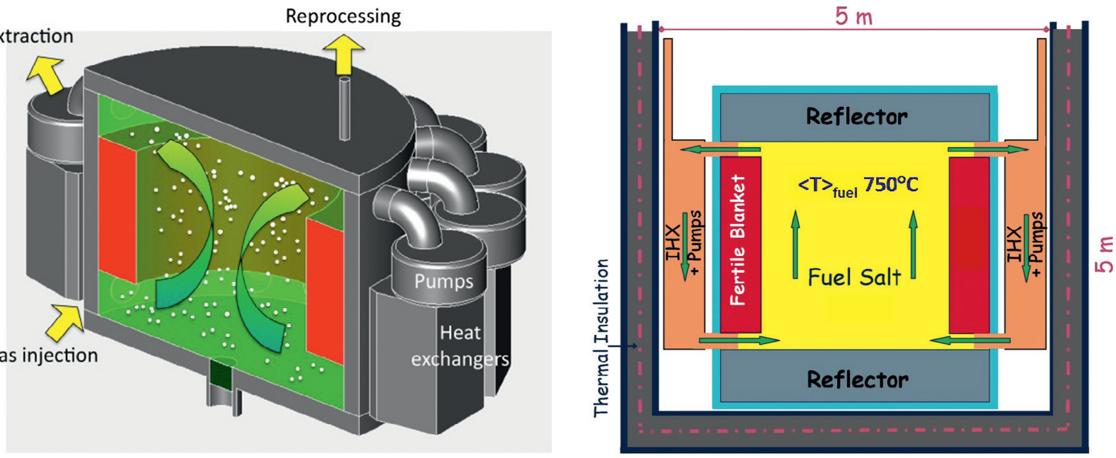

(a) Schematic layout of the reactor **(b) Neutronic model layout**

Fig. 1. Molten Salt Fast Reactor (MSFR).

2. Molten Salt Fast Reactor (MSFR) concept

2.1. System description

The reference MSFR design is a 3000 MWth reactor with three different circuits (or loops) (Rubiolo et al., 2013): the fuel circuit, the intermediate circuit and the power conversion system. The main components of the fuel circuit are: the fuel salt which serves as fuel and coolant, the core, the inlet and outlet pipes, the gas injection system, the salt-bubble separators, the fuel heat exchangers and the pumps. The salt in the fuel loop is made of lithium fluoride and actinide fluoride. The latter is composed by fissile materials (such as uranium 233 and plutonium) and fertile materials (such as thorium). The proportion of heavy nuclei (actinides fluoride) in the fuel salt is fixed at 22.5 mol%. The total fuel salt volume in the fuel loop is about 18 m^3 and the mean salt temperature was set to about 675 °C. As shown in the schematic layout of Fig. 1a, the fuel salt flows from bottom to the top of the core cavity. After exiting the core, the fuel salt is fed into 16 groups of pumps and Heat Exchangers (HXs) located around the core (Brovchenko et al., 2012). The fuel salt circulates in the fuel circuit in around 3–4 s. As can be seen in Fig. 1, the entire fuel circuit is contained inside a reactor vessel which acts as a second barrier. Three important components of the core are: (i) the top and bottom neutron reflectors and (ii) the radial fertile blankets (shown in red[1] in Fig. 1) which are part of the radial reflectors. The thick top and bottom reflectors are made of nickel-based alloys and have been designed to absorb more than 99% of the leaking neutrons. The radial reflectors include a fertile blanket of about 50 cm thick to increase the breeding ratio. This blanket is filled with a fertile salt of LiF-ThF4 with initially 22.5 mol% ^{232}ThF4. The radial reflectors are enclosed by a 20 cm thick layer of B_4C, which provides additional neutron protection of the HXs. The fuel circuit includes a salt draining system which can be used for a planned shut down or in case of incident/accident leading to an excessive increase of the temperature in the core. In such situations the fuel salt geometry can be passively reconfigured by gravity draining of the fuel salt into tanks located under the reactor and where a passive cooling and adequate reactivity margin can be obtained.

At earlier stages of the reactor design, in particular for the initial neutronics studies, the MSFR core was approximated as a single compact cylinder of fuel salt (2.25 m high × 2.25 m diameter) as shown in Fig. 1b. At the current stage more detailed and realistic core geometries are being investigated as part of the MSFR thermal–hydraulics design (EVOL FP7 project). As already discussed, two of the requirements of the thermal–hydraulics design are: (i) maximizing the overall flow mixing in the core cavity and (ii) reducing the temperature peaking factors in the salt and on the core walls. These two design requirements allow improving the homogeneity of the salt (both in composition and in the content of the inert gas bubbles) and reducing the thermal stress on the walls. A third requirement was added to this list and consists in avoiding the use of a core internal structure. This new requirement was motivated from results of preliminary investigations which used various types of core internals, including perforated plates, flow grids or salt injectors, to obtain an adequate thermal–hydraulic performance. In all cases, it was found that acceptable flow mixing and temperature peaking factors could be obtained but at the price of a significant increase of the pressure losses and then of the fuel salt pumping power. This will adversely impact the design of fuel salt pumps. Moreover, it was observed that hydraulic performance of these structures (in terms of flow mixing) was not as efficient as expected and could be degraded by the reactor flow rate (i.e. it may change with the operating conditions). In addition to this drawback, the use of core internals in the MSFR poses an important number of other challenges. To mention a few of them, in normal operation, corrosion, vibration and radiation damage will be important issues that need to be addressed to ensure the integrity of the structure. The possibility of a partial blockage will have to considered, the core internals inspection and maintenance operations will be also difficult. During incidental/accidental conditions, core internal structures could be severely damaged (or melt) because of the thermal heating (on the contrary core walls can be protected by a thermal-shield and by external cooling). In addition, a core internal could also degrade the performance of the salt draining system and the performance of the reactor natural convection flow. Finally, these structures will difficult the seismic design of the core cavity. For the all these reasons, the idea of using core internals was abandoned and the effort was instead directed to the use of the core walls to obtain an adequate flow distribution. This approach has a relatively small impact on the neutronics performance due to the relatively low importance of the neutron leaks in the MSFR design.

The optimization of the core cavity was performed in several stages, starting by curving the shapes of the radial walls (in contact

[1] For interpretation of color in Fig. 1, the reader is referred to the web version of this article.

with the fertile blanket) to better conform the flow shape in the cavity. Then the inlet and the outlet fuel channels were bended to continue to improve the flow mixing (e.g. to obtain a better spread of the inlet jets) and to reduce the potential flow recirculation or dead zones. It was finally noticed, that curving the core bottom and top walls will further reduce the volume of the recirculation zones that appear in the lower part of the cavity. Reduction of this recirculation zone decreases the temperature radial gradient. A number of geometries were analysed, however for simplicity this paper discusses only the two which exhibit the best thermal–hydraulics performance. These two geometries, called here Geometry I and Geometry II, are shown in Fig. 2 and have the following characteristics:

- Geometry I: as shown on the left side of Fig. 2, the radial core walls (in contact with the fertile blanket) of this geometry have a curved shape. Note that while the bottom core wall (bottom reflector) is straight the top core wall (top reflector) is curved to reduce the wall maximum temperature. While detailed modelling of this geometry usually requires a 3D CFD model, a less computing demanding 2D model (assuming a radial symmetry) was also used and compared against the 3D model.
- Geometry II: as shown on the right side of Fig. 2, in the Geometry II all core cavity walls are symmetrically curved in an attempt to further improve the flow distribution and avoid too large temperature hot spots on the upper wall. Only a 3D model of this geometry was used in the analysis.

In the CFD analysis of Geometry I, the study domain using the 2D model is limited to the core cavity, the core inlet and outlets (see Fig. 3a). The presence of the fuel salt pumps and the HXs are taken into account only through the boundary conditions (inlet flow and outlet pressure). On the contrary, in the 3D models (for both Geometries I and II), the CFD domain includes the entire fuel circuit as shown in Fig. 2. The HXs are modelled as a porous medium and the pumps as an impulsion force that allows obtaining the reactor nominal flow rate. In all cases, the MSFR bubbling system used for fission product reprocessing is not considered since under normal conditions it effects on the salt flow are negligible. Both heat generation arising from the fission reaction and decay heat are included in the heat source while the thermal power in the blanket is neglected (see Section 3).

2.2. Fuel salt thermodynamic properties

Consistently with the current MSFR configuration, a binary fluoride salt, composed of LiF enriched in ^{7}Li to 99.995 mol% and 22.5 mol% of heavy nuclei has been used as working fluid in the CFD simulations. While during reactor operation, fission products and new heavy nuclei are produced in the salt up to some few mol%, they do not impact the salt thermodynamic properties used in these studies. The fuel salt properties are considered then as unchanged over time and equal to those of the initial fuel load. The experimental determined correlations employed to calculate these properties are given in Table 1 (Delpech et al., 2009). The fuel salt melting temperature is equal to 838 K (565 °C).

3. Methodology

3.1. Model equations

As previously discussed two different geometries were considered in the analysis: Geometry I and Geometry II. The first geometry was studied using 2D and 3D models. Although a one-sixteenth core model could be used for the 3D model in order to reduce the computational effort, a one-quarter model (as illustrated in Fig. 2) was instead employed because it will allow performing future studies on non-symmetric reactor flow conditions such as those encountered after the stop of a fraction of the fuel salt pumps. Potential flow patterns and/or instabilities may also involve more than one reactor loop and then a one-quarter model would be better to detect their presence.

The model equations were solved assuming that steady turbulent flow conditions exist in the reactor. This is indeed the case in many practical situations (and also suitable for the MSFR), where the flow is steady in the mean i.e. while unsteady turbulent fluctuations exist the time averaged velocity field appears to be steady. The numerical resolution of the flow mass, linear momentum and energy balance equations was carried out in two different manners: (i) using steady simulations by neglecting the governing equations' time derivatives and (ii) performing a transient simulation which take into account the equations' time derivatives. Since the problem variables (reactor thermal power and boundary conditions) are assumed to have a constant value, both approaches should converge to the same solution provided that turbulent

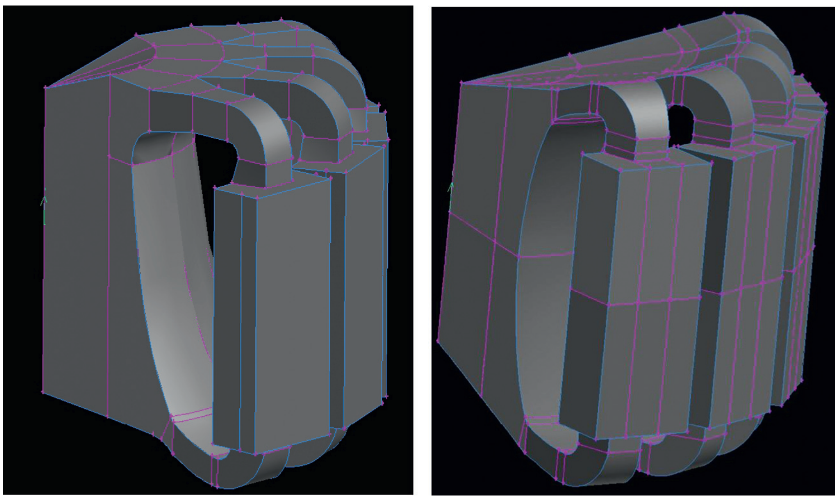

(a) Geometry I (b) Geometry II

Fig. 2. MSFR core geometries used in the CFD thermal–hydraulics studies.

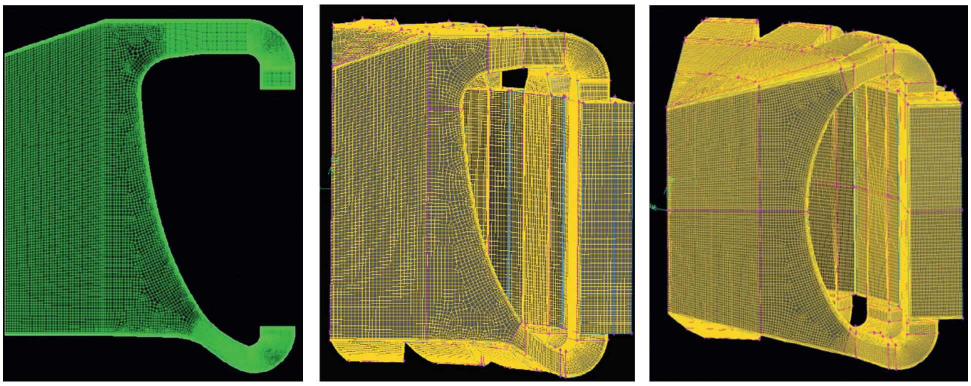

(a) 2D model for Geometry I (b) 3D model for Geometry I (c) 3D model for Geometry II

Fig. 3. CFD meshes used in the thermal–hydraulics studies. The HXs shown in the 3D geometry are approximated in the CFD study as a porous medium.

Table 1
Physicochemical properties of the fuel salt as a function of its temperature *T* in *K*.

		Unit	Formula	A	B	Validity range (K)
Specific heat capacity	C_p	J/K/kg	A + BT	−1111	2,78	[867–907][a]
Thermal conductivity	λ	W/K/m	A + BT	0.928	8.40E−05	[891–1020]
Density	ρ	kg/m^3	A + BT	4983.56	−0.882	[893–1123]
Dynamic viscosity	μ	Pa s	$\rho \cdot A \cdot \exp(B/T)$	5.55E−08	3689	[898–1119]

[a] Note that the specific heat capacity is extrapolated beyond 907 K.

steady conditions exist in the reactor. The results of the simulations seem to support this assumption since the presence of flow instabilities (transient flow) can be detected sometimes because of the poor numerical convergence of the CFD simulations that they cause. This was not the case in the simulations presented in this paper where a good convergence was found thus supporting the assumption of steady turbulent flow conditions for the two proposed geometries. On the contrary, in other geometries (not discussed here) a bad numerical convergence was sometimes observed which may indicate the existence of flow transients. At a more advance phase of the reactor design, it would be suitable to perform transient calculations using a more detailed description of the reactor (for instance including the detailed HX's design). At the present stage, where various core geometries were investigated this will be prohibited.

3.1.1. Conservation of mass, linear momentum and energy

Assuming a constant salt density ρ_o the averaged mass conservation equation (continuity equation) is simplified as follows:

$$\frac{\partial \bar{u}_j}{\partial x_j} = 0$$

In the case of steady turbulent flow then $\bar{u}_j$ is the time averaged value of the j component of the fuel salt velocity. If the flow is not turbulent steady (transient flow), the time averaging has to be replaced by the ensemble averaging. As can be seen in Table 1, the salt density varies in function of the temperature. However, the constant salt density approximation (thus incompressible flow) still provides a good accuracy for our applications as long as the effects of the fuel salt density variations in the gravity force are taken into account through the Boussinesq approximation. In addition, comparison between simulations using incompressible flow equations (with the Boussinesq approximation) and compressible flow equations did not show significant differences.

The momentum conservation equations were solved using the Navier Stokes equation with the RNG (ReNormalization Group) k-epsilon turbulence model:

$$\frac{\partial \bar{u}_i}{\partial t} + \frac{\partial}{\partial x_j}(\bar{u}_j \bar{u}_i) = -\frac{\partial}{\partial x_i}\left(\frac{\bar{p}}{\rho_o} + \frac{2}{3}k\right) + \frac{\partial}{\partial x_j}\left\{(\upsilon + \upsilon_t)\left[\left(\frac{\partial \bar{u}_i}{\partial x_j} + \frac{\partial \bar{u}_j}{\partial x_i}\right) - \frac{2}{3}\left(\frac{\partial \bar{u}_k}{\partial x_k}\right)\delta_{ij}\right]\right\} + g_i[1 - \beta(\bar{T} - T_o)]$$

where $\bar{p}$ is the time averaged fluid pressure, υ the kinematic viscosity, υ_t the turbulent viscosity, g_i the i component of the gravity acceleration, k the turbulent kinetic energy, β the salt expansion coefficient, $\bar{T}$ the salt time averaged temperature and T_O a reference temperature (for example the inlet temperature). The equation uses the Boussinesq approximation, i.e. only the gravitational force takes into account the effects of the density variation through the salt expansion coefficient. Both υ_t and k are calculated according to the RNG k-epsilon turbulence model whose characteristics can be found in the literature (for example in Bird et al., 2002; Shih et al., 1995). At the current stage of the MSFR design, a « RANS » model (Reynolds Average Navier Stokes) provides a good compromise between the precision required for the thermal–hydraulics design, the computational effort and the number of scoping studies that are needed. Moreover, some prospective studies have confirmed that for Reynolds number over 50,000, the results precision of RNG k-epsilon model is quite good. During the next stage of thermal–hydraulics studies a more precise turbulence model such as a LES approach and a comparison against an experimental benchmark would be suitable.

Without introducing a significant error, an assuming incompressible flow, the fuel salt energy conservation equation can be approximated as follows:

$$\frac{\partial \bar{T}}{\partial t} + \frac{\partial}{\partial x_j}(\bar{T}\bar{u}_j) = k_{eff}\frac{\partial}{\partial x_k}\left(\frac{\partial \bar{T}}{\partial x_k}\right) + S$$

where $\bar{T}$ the salt time averaged temperature and

$$k_{eff} = \frac{\upsilon_t}{\mathrm{Pr}_t} + \frac{\upsilon}{\mathrm{Pr}}$$

The salt Prandtl number Pr and other salt thermodynamic properties are calculated using the correlations described in Section 2.2. The turbulent Prandtl number Pr_t is determined from the turbulent viscosity and conductivity which are computed from *k*-epsilon equations. The energy released by the fission reaction and the decay heat from the fission products and actinides is represented by the volumetric heat source number *S*. Under steady reactor operation, the heat source *S* depends only on the spatial position and can be determined from the neutronic simulations as discussed in the next section.

3.1.2. Heat source

Constant nuclear power generation were considered in the simulations. The heat source *S* takes into account the energy released by the fission reaction and the decay heat from the fission products and the actinides. The fission source was estimated from neutronics simulations. These simulations were performed using the Monte Carlo N-Particle code (MCNP) which evaluates the neutron flux and the reaction rates in the simulated system. For simplicity the reference neutron core geometry was used for these studies rather than the different variants of the geometries used in the thermal–hydraulics studies. The fission heat source was later adapted to the actual thermal–hydraulics geometry by using a geometrical homothetic transformation. The functional dependency of the source *S* with the position depends then on the core cavity shape and it is rather complicate. As an example for the Geometry I the heat source is:

$$S = A\ \cos\left(\frac{\pi}{2}\cdot\frac{r_n}{r_o}\right)\cos\left(\frac{\pi}{2}\cdot\frac{z}{z_o}\right)$$

and

$$r_n = \begin{cases} r(1.05550 + 0.228960z) & z \leqslant 0.59\ \text{m} \\ r(1.40277 - 0.359622z) & z > 0.59\ \text{m} \end{cases}$$

where $[S] = \text{W/m}^3$, $A = 7.8381690710^8\ \text{W/m}^3$, $r_o = 1.671773$ m and $z_o = 1.8744$ m.

It is interesting to note that due to fissions of the ^{233}U, a heat source exists in the fertile salt contained in the blanket surrounding the core. This heat source has been estimated to be about 25 MW, and thus much smaller than the heat source arising from nuclear fission in the fuel salt. The blanket heat source can then be neglected for the purpose of the core thermal–hydraulics studies but should be considered for the design of the blanket cooling system.

3.1.3. Boundary conditions

In the 2D model, the CFD study domain includes the core cavity, the core inlet and outlets. The presence of the fuel salt pumps and the HXs are not explicitly modelled but taken into account through the model inlet conditions. In the 3D models, the CFD domain includes the entire fuel circuit geometry (i.e. it is a close loop). The HXs are modelled as a porous medium and the fuel salt pumps as an impulsion force in the fluid of that region that allows obtaining the nominal flow rate in the reactor. In all models (2D and 3D), the MSFR bubbling system used for fission product reprocessing is not considered in the analysis since under normal conditions it effects on the salt flow are negligible. The following conditions were used in the simulations:

- Core operating conditions
  (a) Total flow rate of 18932.2 kg/s (for the full core) which corresponds to 1183.3 kg/s in each exchanger (then for each injection). The resulting average inlet velocity is 3.987 m/s for the 3D models and 1.577 m/s for 2D model of the Geometry I. In the 2D model, this condition was introduced as a uniform inlet velocity (after the HXs), turbulent intensity was set to 5% and the hydraulic diameter to 0.27 m. In the 3D models, the pump impulsion was adjusted such as obtaining the appropriate flow rate in the leg. In the 3D model the velocity profile at the core inlet is not uniform (depending on the mixing in the HXs) but the average value is the nominal one (3.987 m/s).
  (b) Inlet core fuel salt temperature was setup equal to 625 °C which provides an approximate core mean temperature of 675 °C consistent with the salt temperature used in neutronics calculations. In the 2D model, this condition was introduced by setting a uniform inlet temperature (after the HXs). In the 3D models, the heat transfer in the HXs was tuned to obtain the reference average inlet temperature of 625 °C. A small temperature heterogeneity may exist in the core inlet depending on the HXs.
- Core outlet conditions (pump inlet): relative pressure was set equal to 0 Pa
- Bottom and top reflectors and blanket walls
  (a) Non-slip conditions with a wall function for turbulence model that assumes a small wall roughness (which corresponds to an hypothesis of a roughness height smaller than 40–50 μm).
  (b) Adiabatic wall (no heat flux). As previously discussed, the blanket heat source is about 25 MW and thus negligible with respect to the 3000 MW source in the core. Therefore the blanket heat source does not significantly contribute to heat up the salt flow in the core. For the top and bottom reflectors, the adiabatic wall assumption implies that the heat leak is negligible compare to the total power. This assumption is conservative since they will lead to a slightly overestimate of the wall temperature.

3.2. CFD model mesh

The mesh characteristics were chosen to obtain a good balance between convergence and precision (of the temperature and velocity gradients), and the computing effort. At this stage of the reactor design, this last constraint is important since various core geometries have to be investigated. The maximum bulk cell size is comprised between 2 and 3 cm, with a refinement near the core walls with reduce the cell thickness to about 1–2 mm. In order to decrease number of cells a mesh technique by elevation was used: the mesh algorithm created hexahedra from quadrangle surface elements, and prism from triangle surface elements. The full 3D meshes of a quarter of the core contain between 5 and 6 million cells. The meshes used in the Geometry I (2D and 3D models) and in the Geometry II (3D model) are illustrated in Fig. 3.

3.3. CFD code

The version 6.3.26 of FLUENT® CFD code was used in the simulations. FLUENT is a general-purpose computational fluid dynamics software package that can be used to model flow, turbulence, heat transfer, and chemical reactions for industrial applications. The meshes were built with the mesher GAMBIT.

4. Results

This section presents the flow temperature and velocity distribution determined by the CFD calculations, firstly for the 2D and 3D models of Geometry I and then for the 3D model of Geometry II. The analysis of the sensitivity to the reactor operating conditions for this later geometry is also discussed.

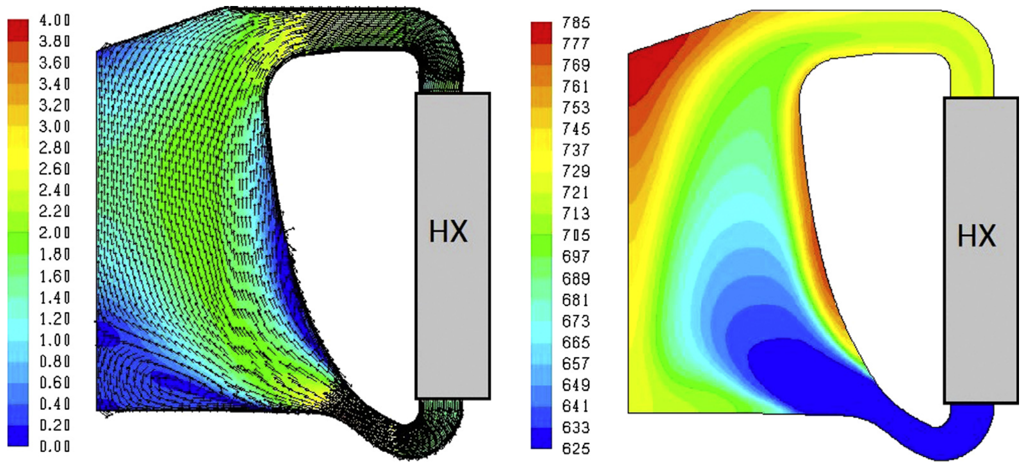

(a) Fuel salt velocity field [m/s] **(b) Fuel salt temperature distribution [°C]**

Fig. 4. CFD predictions for the 2D model (radial symmetry) of Geometry I.

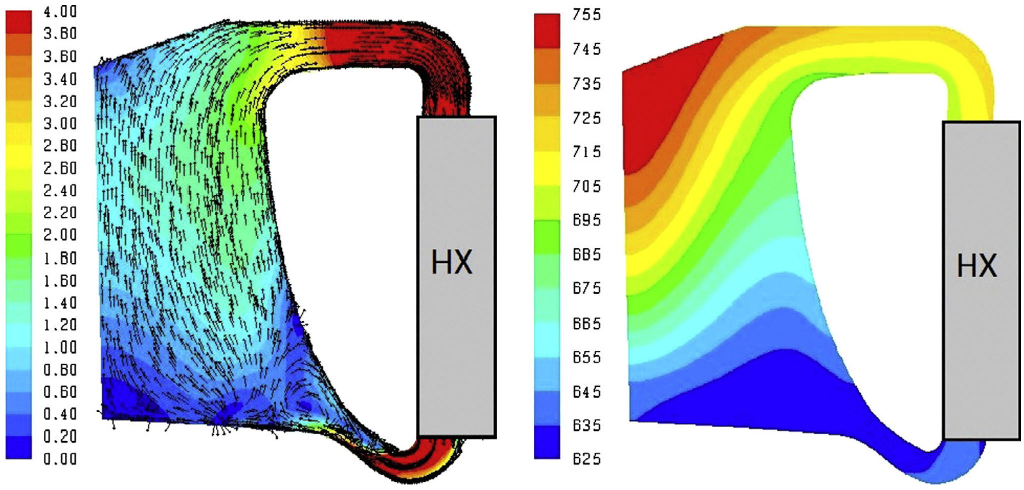

(a) Fuel salt velocity field [m/s] **(b) Fuel salt temperature distribution [°C]**

Fig. 5. CFD predictions for the 3D model of Geometry I.

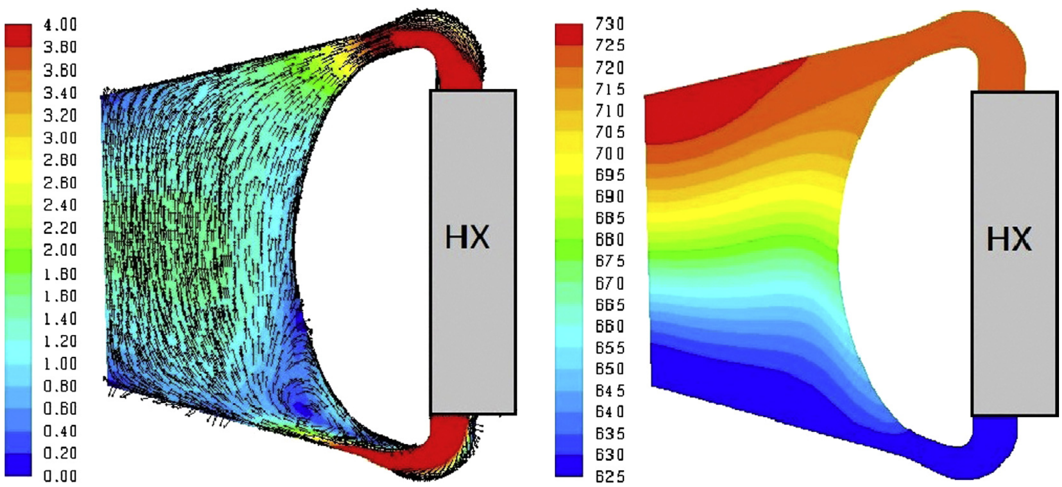

(a) Fuel salt velocity field [m/s] **(b) Fuel salt temperature distribution [°C]**

Fig. 6. CFD predictions for the 3D model of Geometry II.

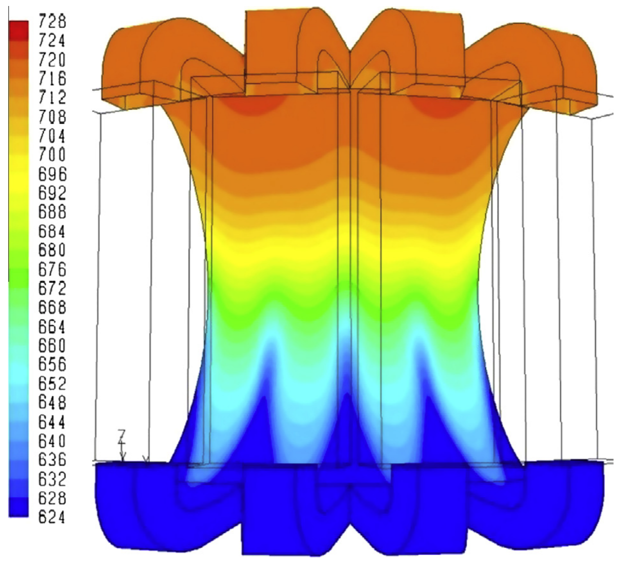

Fig. 7. Temperature [°C] in a symmetry plane of an inlet/outlet and on the walls.

4.1. Results obtained for the 2D and 3D models of the Geometry I

The fuel salt velocity distribution and temperature fields for the 2D and 3D models of the Geometry I are presented in Figs. 4 and 5 respectively. The average velocities in the inlet and outlet legs of the 2D model are smaller than in the 3D model. This is due to the radial symmetry condition used in the 2D model (and thus the inlet/outlet sections in the 2D model are larger than in the 3D model). In both the 2D and 3D models, the maximum velocity occurs near the bottom reflector due to the curvature of the inlet. Then the flow goes up, with a small stagnation zone near the outer wall (fertile blanket) and a more or less flat velocity profile in the central part of the core. Generally speaking, the predicted flow is more uniform in the 3D model probably due to 3D mixing effects in the inlet zone.

In the 2D model and as can be seen in Fig. 4b, the temperature distribution is more heterogeneous due to the inlet jet. A better mixing is observed in Fig. 5b for the 3D model which allows obtaining a better thermal homogeneity in the core bottom. The hottest temperature is still on the stagnation point on top reflector and on blanket wall. The highest temperature is about 785 °C in 2D and about 750 °C in 3D, which correspond to 60 °C/30 °C above the average outlet temperature. As it will be discussed in the next section, the Geometry II allows for the suppression of hot spots near the blanket and the bottom reflector. Finally, the comparison (not shown here) between CFD simulations assuming incompressible flow with and without taking into account the effect of the salt density variations in the gravity force (buoyancy force) shows relatively small changes on the size and the temperature distribution of the recirculation zones. The overall direction of the flow rotation in the recirculation zones is not compatible with a thermal convection effect as can be seen in Fig. 4 or 5.

From these results it can be concluded that while the 2D model does not predict the same velocity and temperature distributions of the more precise 3D model, its accuracy is still sufficient for performing prospective thermal studies which may involve a large number of simulations.

4.2. Results obtained for the 3D model of the Geometry II

The fuel salt velocity and temperature distributions for the symmetrical curved wall geometry (3D) are presented in Fig. 6. A 3D view of the core wall temperature is presented in Fig. 7. As can be seen, the Geometry II allows obtaining a more uniform velocity distribution with relatively small temperature radial gradients which minimizes the salt hot spot. The flow velocity and temperature distribution are more symmetrical than those obtained for the Geometry I. Note that a small flow recirculation remains near the inlet (bottom right of Fig. 6a) but globally the salt flow velocity field is more uniform than for the Geometry I. More important, the effectiveness of this geometry is shown on temperature field: the maximum temperature is only 6° over the average outlet temperature (Fig. 6b) and the temperature is almost homogeneous in the radial direction even though the heat source varies with the radius. The only regions were a significant radial temperature gradient exists is near the core inlet due to the injection jets (see Fig. 7).

From these results it was concluded that Geometry II allows obtaining a very acceptable temperature distribution. Moreover, as it will be discussed in the next section, preliminary studies show that the temperature and velocity distributions are relatively

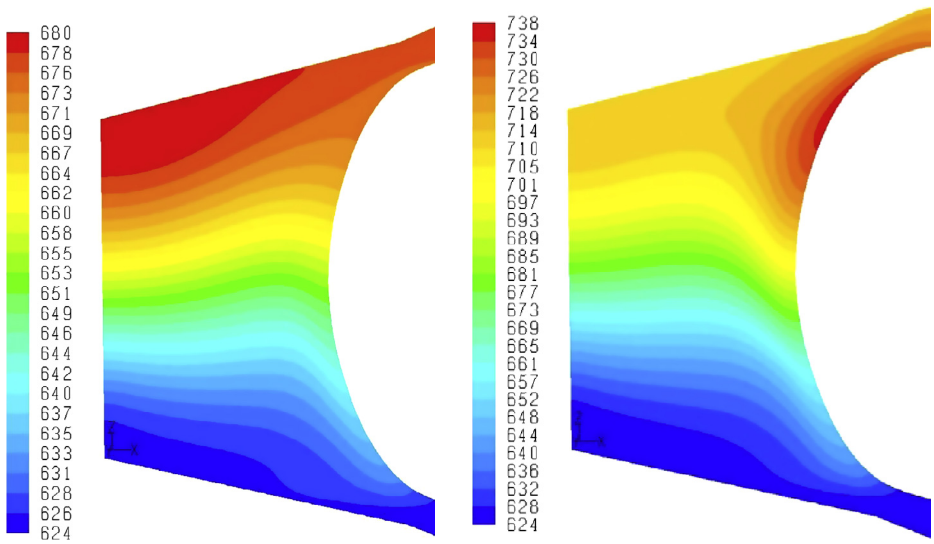

(a) Case 1: half power and nominal flow rate **(b) Case 2: half power and half flow rate**

Fig. 8. Temperature distribution [°C] at two different reactor working conditions (Geometry II 3D model.

Table 2
Summary of the results of the sensitivity study to reactor operating parameters (Geometry II 3D model).

	Reference case	Case 1	Case 2
Heat source (GW)	2,7959	1,398	1,398
Mass flow rate (kg/s)	18923,2	18923,2	9461,6
T_out (°C)	722	676	722
T_out–T_in (°C)	97	51	97
Pressure drop core (bar)	~0.1	~0.1	~0.03
T_max–T_out (°C)	6	4	16
Tmax_walls (°C)	728	680	738

stable and show a small sensitivity to the system parameters such as the reactor working conditions, salt properties, heat source, etc.

4.3. Sensitivity to the working point

The sensitivity of the flow velocity and temperature distributions of the symmetrical curved wall geometry (3D model) to some of the problem parameters is discussed in this section. In particular, the two following cases were investigated:

- Case 1: The reactor power was reduce to half of the nominal value (the heat source spatial distribution remains unchanged),
- Case 2: A reduction of both the reactor power and the total flow rate to half of their nominal values.

As shown in Fig. 8a, in Case 1, the velocity and temperature fields are similar to the nominal conditions case. The maximum core outlet temperature decreases to 676 °C and the hot spot temperature to 680 °C. The hot spot is still in the centre of the top wall of the core. In the second case (half power and half total flow rate) the differences are more important (see Fig. 8b): the hottest point is now the top part of the blanket wall with a temperature 16° over average outlet temperature. The stagnation point (centre of top reflector) is now cooler than the outlet. The homogeneity is then degraded with respect to the reference conditions, radial temperature gradient is more than two times higher and the highest temperature is about 738 °C. Nevertheless, the homogeneity is still quite good. All these results are summarized in Table 2.

5. Conclusions

A thermal–hydraulic study of the core of the Molten Salt Fast Reactor (MSFR) has been presented. The numerical simulations were carried-out using a Computation Fluid Dynamic code. The main objective of these calculations was to optimize the reactor core geometry in order to minimize the temperature peaking factors. The CFD results showed that a core cavity with a curved walls and inlet/outlet legs (called Geometry II in this paper) allows obtaining a relatively uniform temperature distribution without using any lower core internals (such as a perforated plate) to improve flow mixing. The simulations results show a very good thermal homogeneity: the hottest point is less than 10 °C above the average outlet temperature and is located in the centre of the top wall of the core. The CFD results show also a moderate sensitivity of these results to the working point. Future CFD studies will be focused on further investigating the temperature distribution sensitivity to the reactor parameters and on improving the accuracy of the numeric predictions by performing a direct coupling with the neutronics simulations.

Acknowledgments

The authors wish to thank the PACEN (Programme sur l'Aval du Cycle et l'Energie Nucléaire) and NEEDS (Nucléaire : Energie, Environnement, Déchets, Société) programs of the French Centre National de la Recherche Scientifique (CNRS), the IN2P3 department of CNRS, and the European program EVOL (Evaluation and Viability of Liquid Fuel Fast Reactor System) of FP7 for their support.

References

Bettis, E.S. et al., 1970. The design and performance features of a single-fluid molten-salt breeder reactor. Nucl. Appl. Technol. 8, 190–207.
Bird, R.B., Stewart, W.E., Lightfoot, E.N., 2002. Transport Phenomena, second ed. J. Wiley & Son, NY.
Brovchenko, M. et al., 2012. Preliminary safety calculations to improve the design of molten salt fast reactor. In: Proceedings of the International Conference PHYSOR 2012 Advances in Reactor Physics Linking Research, Industry, and Education, Knoxville, Tennessee, USA.
Delpech, S., Merle-Lucotte, E., Heuer, D., et al., 2009. Reactor physics and reprocessing scheme for innovative molten salt reactor system. J. Fluorine Chem. 130 (1), 11–17.
Forsberg, C.W. et al., 2007. Liquid salt applications and molten salt reactors. Rev. Gén. Nucl. 4/2007, 63.
GIF (Generation IV International Forum), 2008, Annual report 2008. http://www.gen-4.org/PDFs/GIF_2008_Annual_Report.pdf. pp. 36–41.
Mathieu, L., Heuer, D., et al., 2006. The thorium molten salt reactor: moving on from the MSBR. Prog. Nucl. Energy 48, 664–679.
Mathieu, L., Heuer, D., Merle-Lucotte, E., et al., 2009. Possible configurations for the thorium molten salt reactor and advantages of the fast non-moderated version. Nucl. Sci. Eng. 161, 78–89.
Merle-Lucotte, E., Heuer, D. et al., 2008. Introduction of the physics of molten salt reactor, materials issues for generation iv systems. NATO Science for Peace and Security Series – B, Editions Springer, pp. 501–521.
Merle-Lucotte, E., Heuer, D. et al., 2009. Minimizing the fissile inventory of the molten salt fast reactor. In: Proceedings of the Advances in Nuclear Fuel Management IV (ANFM 2009), Hilton Head Island, USA.
Nuttin, A., Heuer, D., et al., 2005. Potential of thorium molten salt reactors. Prog. Nucl. Energy 46, 77–99.
Rubiolo, P., Heuer, D., et al., 2013. Overview and perspectives of the molten fast salt reactor (MSFR) concept. In: Proceedings of the Conference on Molten Salts in Nuclear Technology (CMSNT-2013). Bhabha Atomic Research Centre, Mumbai, India.
Shih, T.-H., Liou, W.W., et al., 1995. A new k–ε eddy-viscosity model for high reynolds number turbulent flows – model development and validation. Comput. Fluids 24 (3), 227–238.
US DOE nuclear energy research advisory committee and the generation iv international forum, 2002. A Technology Roadmap for Generation IV Nuclear Energy Systems, GIF-002-00.
Whatley, M.E. et al., 1970. Engineering development of the MSBR fuel recycle. Nucl. Appl. Technol. 8, 170–178.